

Preparation and Characterization of Spherical $\text{Li}_3\text{V}_2(\text{PO}_4)_3/\text{C}$ Cathode Material for Lithium-ion Batteries

G. Yang^{1,*}, J. R. Ying^{1,2,*}, J. Gao¹, C. Y. Jiang¹ and C. R. Wan¹

¹Institute of Nuclear and New Energy Technology, Tsinghua University, P.O. Box 1021, Beijing 102201, P. R. China

²Institute of Chemical Engineering, Ningbo University of Technology, 89 Cuibai Road, Ningbo 315016, Zhejiang Province, P. R. China

Received: November 3, 2008, Accepted: August 29, 2009

Abstract: Monoclinic lithium vanadium phosphate $\text{Li}_3\text{V}_2(\text{PO}_4)_3$ is a very promising polyanion-type cathode material for lithium-ion batteries. In this work, we synthesized spherical $\text{Li}_3\text{V}_2(\text{PO}_4)_3$ powder via melting V_2O_5 and quenching followed by spray drying and carbothermal reduction processes, using NH_4VO_3 , $\text{LiOH}\cdot\text{H}_2\text{O}$, H_3PO_4 and $\text{C}_{12}\text{H}_{22}\text{O}_{11}$ as the raw materials. The structure and morphology of the $\text{Li}_3\text{V}_2(\text{PO}_4)_3$ powders were characterized. The electrochemical property of the spherical $\text{Li}_3\text{V}_2(\text{PO}_4)_3$ cathode material was characterized by electrochemical measurements. At cut-off voltages of 3.0–4.3 V, 3.0–4.8 V and 1.5–4.8V with current density of $0.2 \text{ mA}\cdot\text{cm}^{-2}$, the cathode material showed initial discharge capacity of $124.7 \text{ mAh}\cdot\text{g}^{-1}$, $157.3 \text{ mAh}\cdot\text{g}^{-1}$, $270.2 \text{ mAh}\cdot\text{g}^{-1}$ and capacity retention of 98.4%, 83.1% and 84.0% after 50 cycles, respectively. The charge-discharge performance tested at different current densities of $0.04 \text{ mA}\cdot\text{cm}^{-2}$, $0.08 \text{ mA}\cdot\text{cm}^{-2}$, $0.2 \text{ mA}\cdot\text{cm}^{-2}$, $0.4 \text{ mA}\cdot\text{cm}^{-2}$, $0.8 \text{ mA}\cdot\text{cm}^{-2}$ and $2 \text{ mA}\cdot\text{cm}^{-2}$ also showed the good rate capability.

Keywords: Lithium secondary batteries; $\text{Li}_3\text{V}_2(\text{PO}_4)_3$; Spray-dried; Spherical

1. INTRODUCTION

Currently, LiCoO_2 is widely used in commercial lithium-ion batteries as the cathode material, but its high cost, unsafety and toxicity prohibit it to be used in large-scale applications [1]. The increasing demand for electric vehicles promotes the development of advanced lithium-ion batteries with high safety, high energy density, long cycle life, etc. Since the demonstration of reversible electrochemical lithium insertion-extraction for LiFePO_4 in 1997 [2], lithium transition metal phosphates have attracted great interest as new promising cathode materials. Compared with LiCoO_2 , the phosphates exhibit remarkable electrochemical and thermal stability.

Recently, the monoclinic lithium vanadium phosphate $\text{Li}_3\text{V}_2(\text{PO}_4)_3$ has been proposed as a cathode material for lithium-ion batteries [3–10]. It has the space group P21/n and crystallizes in a structure with corner-shared VO_6 octaheders and PO_4 tetraheders. At voltages higher than 3.0 V, Li is extracted from $\text{Li}_3\text{V}_2(\text{PO}_4)_3$ through four redox phenomena at about 3.59, 3.67, 4.06 and 4.55 V vs. Li, corresponding to a theoretical capacity of

$197 \text{ mAh}\cdot\text{g}^{-1}$. In addition, $\text{Li}_3\text{V}_2(\text{PO}_4)_3$ shows four reversible redox phenomena upon insertion of two Li^+ at 1.98, 1.88, 1.73 and 1.70 V vs. Li, corresponding to a theoretical capacity of $131 \text{ mAh}\cdot\text{g}^{-1}$ at charge-discharge cut-off voltages of 1.5–3.0 V. In theory, five lithium ions can be reversibly inserted and extracted from the $\text{Li}_x\text{V}_2(\text{PO}_4)_3$ lattice, and the final products are $\text{Li}_5\text{V}_2(\text{PO}_4)_3$ and $\text{V}_2(\text{PO}_4)_3$, respectively. The valence of vanadium in different products can be +2, +3, +4 and +5. Therefore, over the whole range of charge-discharge voltages (1.5–4.8 V), the $\text{Li}_3\text{V}_2(\text{PO}_4)_3$ cathode material has the theoretical specific capacity of $328 \text{ mAh}\cdot\text{g}^{-1}$, which is the highest energy density among the metal phosphates reported. It also possesses good Li^+ -ion mobility, excellent stability, and satisfactory safety. These advantages suggest that $\text{Li}_3\text{V}_2(\text{PO}_4)_3$ can be a commercially useful positive electrode material.

As has been reported, the $\text{Li}_3\text{V}_2(\text{PO}_4)_3$ powders are usually prepared via conventional solid state reaction of mechanically mixed $\text{NH}_4\text{H}_2\text{PO}_4$, V_2O_5 and Li_2CO_3 . The mixture was sintered at 800–900°C for several hours, using H_2 to reduce the V^{5+} to V^{3+} , or using carbon to reduce the V^{5+} via the carbothermal reduction process. In our laboratory, well crystallized monoclinic $\text{Li}_3\text{V}_2(\text{PO}_4)_3$ with good performance has been synthesized via traditional car-

To whom correspondence should be addressed:
Email: *yanggai05@mails.tsinghua.edu.cn, †yingjr@mail.tsinghua.edu.cn
Phone: +86-10-89796085, Fax: +86-10-89796031

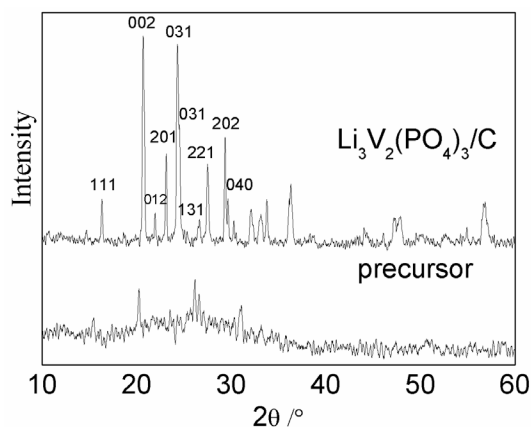


Figure 1. XRD patterns of the spherical precursor and $\text{Li}_3\text{V}_2(\text{PO}_4)_3/\text{C}$ powders.

both thermal reduction method and microwave carbothermal reduction method, using $\text{LiOH}\cdot\text{H}_2\text{O}$, V_2O_5 , H_3PO_4 and sucrose ($\text{C}_{12}\text{H}_{22}\text{O}_{11}$) as raw materials [11,12]. Monoclinic $\text{Li}_3\text{V}_2(\text{PO}_4)_3$ was also synthesized by a sol-gel method. Compared with a solid state reaction method, sol-gel method can mix the starting ingredients at molecular level. It has enormous advantages such as lower calcination temperature, shorter sintering time and smaller particle size of the resulting powder [13-19]. Thus, sol-gel method is a novel concept for the synthesis of an improved $\text{Li}_3\text{V}_2(\text{PO}_4)_3$.

In this work, we synthesized spherical $\text{Li}_3\text{V}_2(\text{PO}_4)_3$ powders via quenching of molten V_2O_5 followed by spray drying and carbothermal reduction processes, using NH_4VO_3 , $\text{LiOH}\cdot\text{H}_2\text{O}$, H_3PO_4 and $\text{C}_{12}\text{H}_{22}\text{O}_{11}$ as the raw materials. The structure, morphology, and electrochemical performance of the spherical $\text{Li}_3\text{V}_2(\text{PO}_4)_3$ cathode material have been investigated in detail.

2. EXPERIMENTAL

First, we used the melt quenching method to prepare V_2O_5 sol. NH_4VO_3 was heated in air atmosphere at 800°C for 2 h. At high temperature, the NH_4VO_3 was decomposed into V_2O_5 and V_2O_5 was melted to obtain liquid V_2O_5 . The liquid V_2O_5 was then quenched into deionized water. The mixture was stirred at room temperature for 4h to obtain V_2O_5 sol. After carefully analyzing the concentration of V_2O_5 in the sol, we added analytically pure $\text{LiOH}\cdot\text{H}_2\text{O}$, H_3PO_4 and sucrose ($\text{C}_{12}\text{H}_{22}\text{O}_{11}$) into the sol in a molar ratio of $\text{LiOH}\cdot\text{H}_2\text{O}:\text{V}_2\text{O}_5:\text{H}_3\text{PO}_4:\text{C}_{12}\text{H}_{22}\text{O}_{11} = 3:1:3:0.2$ and stirred again for 2 h, resulting in the homogeneously mixed sol. The spherical precursor powders containing $\text{LiOH}\cdot\text{H}_2\text{O}$, V_2O_5 , H_3PO_4 and $\text{C}_{12}\text{H}_{22}\text{O}_{11}$ were obtained from the mixed sol via a spray drying method. The spherical $\text{Li}_3\text{V}_2(\text{PO}_4)_3$ powders were synthesized by sintering the precursor powders at 800°C for 16 h in a nitrogen atmosphere. During the sintering process, the sucrose in the precursor would pyrolyse at high temperature and produce reductive atmosphere. The V^{5+} in the precursor would be reduced to V^{3+} and $\text{Li}_3\text{V}_2(\text{PO}_4)_3$ was obtained. The residual pyrolytic carbon (as electronic conducting agent) mixed within the $\text{Li}_3\text{V}_2(\text{PO}_4)_3$ particles to form the composite $\text{Li}_3\text{V}_2(\text{PO}_4)_3/\text{C}$. During the sintering, the reactions may be very complex. We assume the carbothermal reaction

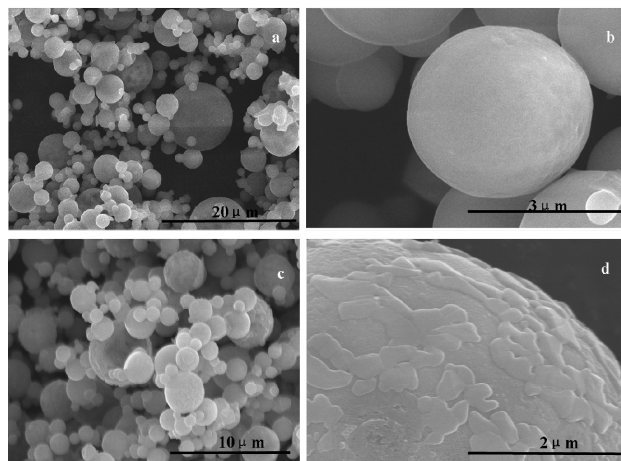
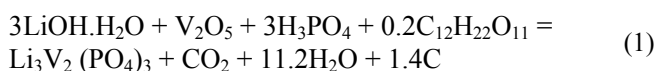


Figure 2. SEM images of the spherical precursor (a), (b) and $\text{Li}_3\text{V}_2(\text{PO}_4)_3/\text{C}$ powders (c), (d).

can be approximately written as the formula below.



According to the formula, the obtained composite will be $\text{Li}_3\text{V}_2(\text{PO}_4)_3/1.4\text{C}$. The calculated residual carbon content is about 4 wt%.

Powder X-ray diffraction (XRD, D/max-rB) with $\text{CuK}\alpha$ radiation was used to identify the crystalline phase and crystal lattice parameters of the powders. The particle morphology, particle size and particle size distribution of the powders were observed using a scanning electron microscopy (SEM, JSM6301F). We also tested the actual carbon content of the $\text{Li}_3\text{V}_2(\text{PO}_4)_3/\text{C}$ powders by dissolving the $\text{Li}_3\text{V}_2(\text{PO}_4)_3/\text{C}$ in diluted HNO_3 , filtering, drying and weighing the mass of the residual carbon.

Experimental test cells for electrochemical measurement used the cathode with the composition 80 wt% $\text{Li}_3\text{V}_2(\text{PO}_4)_3/\text{C}$, 10 wt% carbon black, and 10 wt % PTFE. The separator was a Celguard 2400 microporous polypropylene membrane. The electrolyte was 1M LiPF_6 EC+DEC (1:1 by vol.). A lithium metal anode was used in this study. The cells were assembled in a glove box filled with argon gas. The charge-discharge cycling was galvanostatically performed at 20°C and a current density of $0.04\text{ mA}\cdot\text{cm}^{-2}$, $0.08\text{ mA}\cdot\text{cm}^{-2}$, $0.2\text{ mA}\cdot\text{cm}^{-2}$, $0.8\text{ mA}\cdot\text{cm}^{-2}$ and $2\text{ mA}\cdot\text{cm}^{-2}$ with cut-off voltages of 3.0–4.3 V, 3.0–4.8 V and 1.5–4.8 V (vs Li/Li^+).

3. RESULTS AND DISCUSSION

Fig. 1 shows the XRD patterns of the spherical precursor and $\text{Li}_3\text{V}_2(\text{PO}_4)_3/\text{C}$ powders. In the XRD pattern of the precursor powders, we can observe some weak diffraction peaks ascribing to V_2O_5 . The strong and sharp peaks on the $\text{Li}_3\text{V}_2(\text{PO}_4)_3/\text{C}$ powders' XRD spectra indicate the product was well crystallized. The peaks can be indexed to the monoclinic structure (space group $\text{P}2_1/\text{n}$). There is no evidence of diffraction peaks for carbon, indicating the residual pyrolytic carbon in the product is amorphous. The absence of the impurities' peaks indicates the product is almost phase pure.

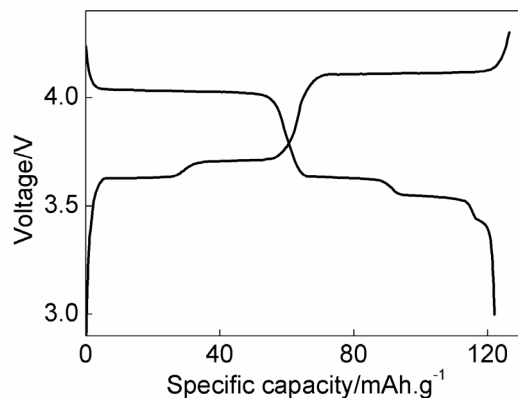


Figure 3. The initial charge–discharge curves of the $\text{Li}_3\text{V}_2(\text{PO}_4)_3/\text{C}$ at 0.2 mA/cm^2 with cut-off voltages of 3.0–4.3 V.

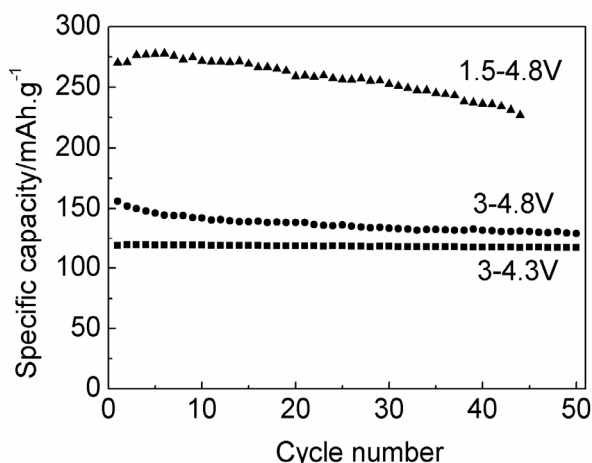


Figure 4. Cycling performance of the $\text{Li}_3\text{V}_2(\text{PO}_4)_3/\text{C}$ at 0.2 mA/cm^2 with different cut-off voltages.

Fig. 2 shows the morphology of the precursor and $\text{Li}_3\text{V}_2(\text{PO}_4)_3/\text{C}$ powders. The powders are both composed of well-dispersed spherical particles. The precursor powders have the particle size distribution of about 1–10 μm . The surface of the spherical precursor particle is smooth and the crystalline grains almost can not be observed. Fig. 2(c) shows after being sintered at 800 $^\circ\text{C}$, the obtained $\text{Li}_3\text{V}_2(\text{PO}_4)_3/\text{C}$ powders are still spherical but shrank obviously, compared to the precursor. The particle size distribution of $\text{Li}_3\text{V}_2(\text{PO}_4)_3/\text{C}$ is about 1–6 μm and mostly is around 2 μm . Each of the spherical particles is made up of a large number of sub-micrometer crystalline grains, as shown in Fig. 2(d). It is tested that the tap-density of the spherical $\text{Li}_3\text{V}_2(\text{PO}_4)_3/\text{C}$ powders is as high as $1.1\text{ g}\cdot\text{cm}^{-3}$, which is higher than that of the irregular $\text{Li}_3\text{V}_2(\text{PO}_4)_3/\text{C}$ powders we prepared before (usually lower than $1.0\text{ g}\cdot\text{cm}^{-3}$). As has been pointed out [20–25], electrode materials composed of spherical particles with appropriate particle size and particle size distribution are expected to have higher tap-density, higher energy density and better manufacturing performance, we believe the spherical $\text{Li}_3\text{V}_2(\text{PO}_4)_3$ should be one of the important directions of this mate-

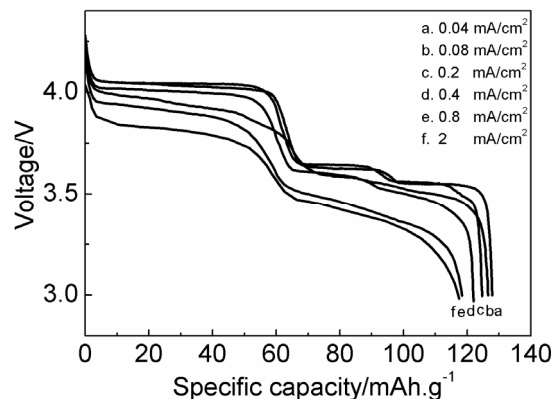


Figure 5. The initial discharge curves of the $\text{Li}_3\text{V}_2(\text{PO}_4)_3/\text{C}$ with cut-off voltages of 3.0–4.3 V at different currents.

rial. By optimizing the melt quenching – spray drying – carbothermal reduction process, the powders' tap-density can be further improved. We will report the results elsewhere.

The actual carbon content of the $\text{Li}_3\text{V}_2(\text{PO}_4)_3/\text{C}$ powders is about 5 wt%, determined by the method described above. The experimental carbon content (5 wt%) is close to the calculated data (4 wt%), indicating the assumed carbothermal reduction equation mentioned in the experimental part is roughly correct.

Fig. 3 shows the initial charge-discharge curves of the $\text{Li}_3\text{V}_2(\text{PO}_4)_3/\text{C}$ at current density of $0.2\text{ mA}\cdot\text{cm}^{-2}$ with cut-off voltages of 3.0–4.3 V. Both curves show three obvious charge-discharge voltage plateaus at around 3.6 V, 3.7 V and 4.1 V. According to Ref. [5], all plateaus correspond to lithium extraction and insertion associated with the $\text{V}^{3+}/\text{V}^{4+}$ redox couple as the first two lithiums of $\text{Li}_3\text{V}_2(\text{PO}_4)_3$ are extracted during charging. The small voltage difference between the charge and discharge plateaus in Fig. 3 shows its good kinetics. The small hysteresis implies high reversibility and a low overvoltage, which confirms the potential suitability of the $\text{Li}_3\text{V}_2(\text{PO}_4)_3$ as an active material for lithium-ion batteries. The cathode material has a first cycle charge capacity of 130.7 mAh/g followed by a discharge capacity of 124.7 mAh/g , giving the rather high initial charge-discharge efficiency of 95.4%. Fig. 4 shows the cycling performance of the $\text{Li}_3\text{V}_2(\text{PO}_4)_3/\text{C}$ at $0.2\text{ mA}\cdot\text{cm}^{-2}$. After 50 cycles, the reversible discharge capacity is $122.7\text{ mAh}\cdot\text{g}^{-1}$, showing the retention of 98.4% of the capacity. Fig. 5 shows the initial discharge curves of the $\text{Li}_3\text{V}_2(\text{PO}_4)_3/\text{C}$ with cut-off voltages of 3.0–4.3V at different currents. At currents density of $0.04\text{ mA}\cdot\text{cm}^{-2}$, $0.08\text{ mA}\cdot\text{cm}^{-2}$, $0.2\text{ mA}\cdot\text{cm}^{-2}$, $0.4\text{ mA}\cdot\text{cm}^{-2}$, $0.8\text{ mA}\cdot\text{cm}^{-2}$ and $2\text{ mA}\cdot\text{cm}^{-2}$, the cathode materials have the initial discharge capacity of $127.9\text{ mAh}\cdot\text{g}^{-1}$, $126.6\text{ mAh}\cdot\text{g}^{-1}$, $124.7\text{ mAh}\cdot\text{g}^{-1}$, $122.0\text{ mAh}\cdot\text{g}^{-1}$, $118.4\text{ mAh}\cdot\text{g}^{-1}$ and $117.4\text{ mAh}\cdot\text{g}^{-1}$, respectively. The excellent cycling performance and rate capability of the $\text{Li}_3\text{V}_2(\text{PO}_4)_3/\text{C}$ cathode material show the material is promising for use in power lithium-ion batteries.

Fig. 6 shows the initial charge-discharge curves of the $\text{Li}_3\text{V}_2(\text{PO}_4)_3/\text{C}$ at current density of $0.2\text{ mA}\cdot\text{cm}^{-2}$ with cut-off voltages of 3.0–4.8 V. On the charge curve, there are four obvious voltage plateaus around 3.6 V, 3.7 V, 4.1 V and 4.6 V. According to Ref. [5], the plateaus around 3.6 V, 3.7 V and 4.1 V correspond

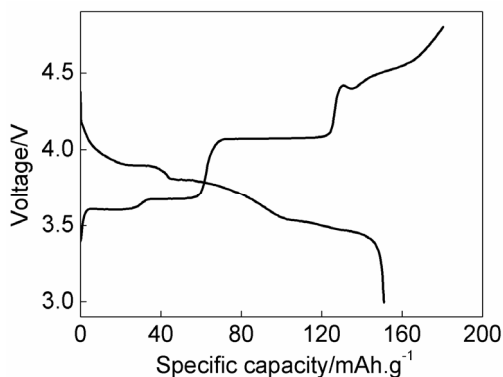


Figure 6. The initial charge–discharge curves of the $\text{Li}_3\text{V}_2(\text{PO}_4)_3/\text{C}$ at 0.2 mA/cm^2 with cut-off voltages of 3.0–4.8 V.

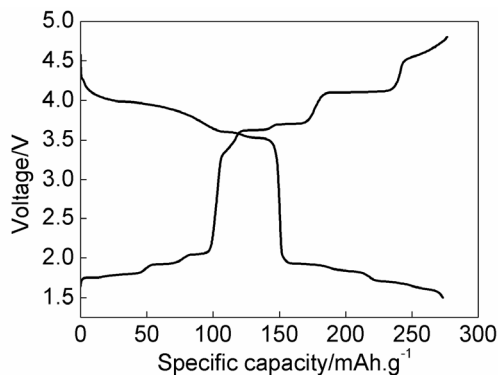


Figure 8. The second charge–discharge curves of the $\text{Li}_3\text{V}_2(\text{PO}_4)_3/\text{C}$ at 0.2 mA/cm^2 with cut-off voltages of 1.5–4.8 V.

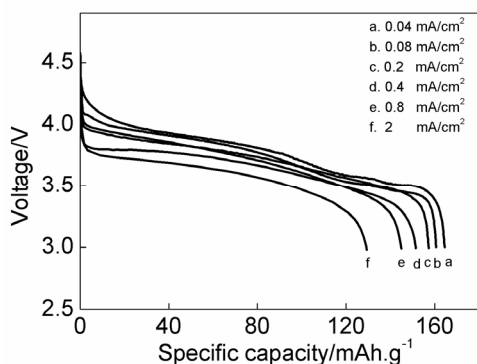


Figure 7. The initial discharge curves of the $\text{Li}_3\text{V}_2(\text{PO}_4)_3/\text{C}$ with cut-off voltages of 3.0–4.3 V at different currents.

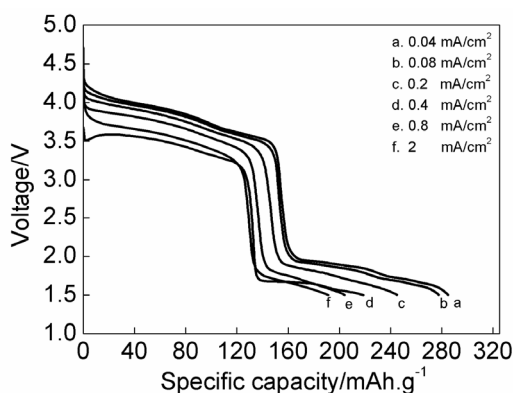


Figure 9. The initial discharge curves of the $\text{Li}_3\text{V}_2(\text{PO}_4)_3/\text{C}$ with cut-off voltages of 1.5–4.8 V at different currents.

to the extraction of the first two lithium ions (the first lithium ion was extracted in two steps). These plateaus are associated with the $\text{V}^{3+}/\text{V}^{4+}$ redox couple. The plateau around 4.6 V corresponds to the extraction of the third lithium ion. It is associated with the $\text{V}^{4+}/\text{V}^{5+}$ redox couple. The cathode material has a first cycle charge capacity of 174.8 mAh/g followed by a discharge capacity of 157.3 mAh/g , and the rather high initial charge–discharge efficiency of 90.0%. Fig. 4 shows the cycling performance of the $\text{Li}_3\text{V}_2(\text{PO}_4)_3/\text{C}$ at $0.2\text{ mA}\cdot\text{cm}^{-2}$. After 50 cycles, the reversible discharge capacity is $130.7\text{ mAh}\cdot\text{g}^{-1}$, showing the retention of 83.1% of the capacity. Fig. 7 shows the initial discharge curves of the $\text{Li}_3\text{V}_2(\text{PO}_4)_3/\text{C}$ with cut-off voltages of 3.0–4.3 V at different currents. At current densities of $0.04\text{ mA}\cdot\text{cm}^{-2}$, $0.08\text{ mA}\cdot\text{cm}^{-2}$, $0.2\text{ mA}\cdot\text{cm}^{-2}$, $0.4\text{ mA}\cdot\text{cm}^{-2}$, $0.8\text{ mA}\cdot\text{cm}^{-2}$ and $2\text{ mA}\cdot\text{cm}^{-2}$, the cathode materials have the initial discharge capacity of $164.5\text{ mAh}\cdot\text{g}^{-1}$, $160.6\text{ mAh}\cdot\text{g}^{-1}$, $157.3\text{ mAh}\cdot\text{g}^{-1}$, $155.3\text{ mAh}\cdot\text{g}^{-1}$, $151.5\text{ mAh}\cdot\text{g}^{-1}$, and $129.4\text{ mAh}\cdot\text{g}^{-1}$, respectively, indicating an excellent rate capability.

Fig. 8 shows the second charge–discharge curves of the $\text{Li}_3\text{V}_2(\text{PO}_4)_3/\text{C}$ at current density of $0.2\text{ mA}\cdot\text{cm}^{-2}$ with cut-off voltages of 1.5–4.8 V. Both of the curves can be divided into three parts. From 3.0 V to 4.8 V, the charge–discharge curves are very similar to the curves illustrated in Fig. 6, corresponding to the $\text{V}^{3+}/\text{V}^{4+}$ and $\text{V}^{4+}/\text{V}^{5+}$ redox couples. From 2.0 V to 3.0 V, the volt-

ages change very sharply with increasing capacity. From 1.5 V to 2.0 V, there should be several steps on the curves, but they are difficult to be distinguished from each other. According to the Ref. [10], two lithium ions can be inserted into $\text{Li}_3\text{V}_2(\text{PO}_4)_3$ to form $\text{Li}_5\text{V}_2(\text{PO}_4)_3$ by discharging to 1.5 V, while the two lithium ions can be extracted reversibly from $\text{Li}_5\text{V}_2(\text{PO}_4)_3$ by charging to 2.0 V. The plateaus correspond to the $\text{V}^{2+}/\text{V}^{3+}$ redox couple. The cathode material has a second-cycle charge capacity of $272.3\text{ mAh}\cdot\text{g}^{-1}$ followed by a discharge capacity of $270.2\text{ mAh}\cdot\text{g}^{-1}$. Fig. 4 shows the cycling performance of the $\text{Li}_3\text{V}_2(\text{PO}_4)_3/\text{C}$ at $0.2\text{ mA}\cdot\text{cm}^{-2}$. After 50 cycles, the reversible discharge capacity is $226.9\text{ mAh}\cdot\text{g}^{-1}$, showing a retention of 84.0% of the capacity. Fig. 9 shows the initial discharge curves of the $\text{Li}_3\text{V}_2(\text{PO}_4)_3/\text{C}$ with cut-off voltages of 1.5–4.8 V at different currents. At current densities of $0.04\text{ mA}\cdot\text{cm}^{-2}$, $0.08\text{ mA}\cdot\text{cm}^{-2}$, $0.2\text{ mA}\cdot\text{cm}^{-2}$, $0.4\text{ mA}\cdot\text{cm}^{-2}$, $0.8\text{ mA}\cdot\text{cm}^{-2}$ and $2\text{ mA}\cdot\text{cm}^{-2}$, the cathode material has the initial discharge capacity of $284.9\text{ mAh}\cdot\text{g}^{-1}$, $277.6\text{ mAh}\cdot\text{g}^{-1}$, $254.9\text{ mAh}\cdot\text{g}^{-1}$, $218.7\text{ mAh}\cdot\text{g}^{-1}$, $204.2\text{ mAh}\cdot\text{g}^{-1}$, and $191.3\text{ mAh}\cdot\text{g}^{-1}$, respectively.

A lot of research work can be done to further improve the electrochemical performance of $\text{Li}_3\text{V}_2(\text{PO}_4)_3$ cathode materials. For example, the substitution of intercalated cations (Li^+), metal cations (V^{3+}), and anion units (PO_4^{3-}) are possible to solve the problem of overvoltage and hysteresis of $\text{Li}_3\text{V}_2(\text{PO}_4)_3$ at high voltage or to

smooth the charge-discharge curves. On the other hand, the tap-density of $\text{Li}_3\text{V}_2(\text{PO}_4)_3$ cathode materials should also be improved.

4. CONCLUSION

Well-crystallized, phase-pure monoclinic lithium vanadium phosphate $\text{Li}_3\text{V}_2(\text{PO}_4)_3/\text{C}$ powders composed of spherical particles have been synthesized via quenching of molten V_2O_5 followed by spray drying and carbothermal reduction processes, using NH_4VO_3 , $\text{LiOH}\cdot\text{H}_2\text{O}$, H_3PO_4 and $\text{C}_{12}\text{H}_{22}\text{O}_{11}$ as the raw materials. This polyanion-type cathode material has excellent electrochemical performance, including broad voltage range, high specific capacity, excellent cycling performance and satisfactory rate capability. Combined with the inherent advantages of phosphates, such as excellent stability and satisfactory safety, the $\text{Li}_3\text{V}_2(\text{PO}_4)_3$ cathode materials are viable candidates for high energy-density and power-demanding lithium-ion batteries.

The new preparation method proposed in this work is suitable to synthesize spherical $\text{Li}_3\text{V}_2(\text{PO}_4)_3/\text{C}$ powders. We expect the new process can be optimized to further improve the cathode material's tap-density and energy-density. Further studies in this field are very promising and significant.

5. ACKNOWLEDGEMENTS

This study is supported by the National Science Foundation of China (Project 50772057), the "973" plan (Project 2007CB209707) and Basic Research Foundation of Tsinghua University (Project JC2007044).

REFERENCES

- [1] A. S. Andersson, J. O. Thomas, *J. Power Sources*, 97, 98 (2001).
- [2] A. K. Padhi, K. S. Nanjundaswamy, J. B. Goodenough, *J. Electrochem. Soc.*, 144, 4 (1997).
- [3] D. Morgan, G. Ceder, M. Y. Saidi, et al., *J. Power Sources*, 119 (2003).
- [4] S. C. Yin, H. Grondey, P. Strobel, et al., *J. Am. Chem. Soc.*, 125 (2003).
- [5] M. Y. Saidi, J. Barker, H. Huang, et al., *J. Power Sources*, 119 (2003).
- [6] S. C. Yin, H. Grondey, P. Strobel, et al., *J. Am. Chem. Soc.*, 125 (2003).
- [7] M. Y. Saidi, J. Barker, H. Huang, et al., *Electrochem. Solid-State Lett.*, 5 (2002).
- [8] J. Barker, R. K. B. Gover, P. Burns, et al., *Electrochem. Solid-State Lett.*, 8 (2005).
- [9] H. Huang, S. C. Yin, T. Kerr, et al., *Adv. Mater.*, 14 (2002).
- [10] S. Patoux, C. Wurm, M. Morcrette, et al., *J. Power Sources*, 119 (2003).
- [11] J. Ying, J. Gao, C. Jiang, et al., *J. Inorg. Mater.*, 21 (2006).
- [12] J. Ying, J. Gao, C. Jiang, et al., *Rare Metal Mat. Eng.*, 35 (2006).
- [13] X. J. Zhu, Y. X. Liu, L. M. Geng, L. B. Chen. *J. Power Sources*, 184, 2 (2008).
- [14] X. J. Zhu, Y. X. Liu, L. M. Geng, L. B. Chen., H. X. Liu, M. H. Cao, *Solid State Ionics*, 179, 27 (2008).
- [15] X. C. Zhou, Y. M. Liu, Y. L. Guo. *Solid State Commun.*, 146, 5 (2008).
- [16] A. P. Tang, X. Y. Wang, Z. M. Liu, *Mat. Lett.*, 62, 10 (2008).
- [17] C. X. Chang, J. F. Xiang, X. X. Shi, X. Y. Han, L. J. Yuan, J. T. Sun, *Electrochim. Acta*, 53, 5 (2008).
- [18] P. Fu, Y. M. Zhao, Y. Z. Dong, X. N. An, G. P. Shen, *Electrochim. Acta*, 52, 3 (2006).
- [19] P. Fu, Y. M. Zhao, Y. Z. Dong, X. N. An, G. P. Shen. *J. Power Sources*, 162, 1 (2006).
- [20] J. Ying, M. Lei, C. Jiang, et al., *J. Power Sources*, 158 (2006).
- [21] J. Ying, C. Jiang, C. Wan, et al., *J. Power Sources*, 129 (2004).
- [22] J. Ying, C. Wan, C. Jiang, et al., *J. Power Sources*, 99 (2001).
- [23] J. Gao, C. Jiang, J. Ying, et al., *J. Power Sources*, 155 (2006).
- [24] J. Gao, C. Jiang, J. Ying, et al., *J. Inorg. Mater.*, 20 (2005).
- [25] J. Ying, J. Gao, C. Jiang, et al., *J. Inorg. Mater.*, 21 (2006).